ELSEVIER

Chemical Engineering Journal 138 (2008) 55–62

Chemical Engineering Journal

www.elsevier.com/locate/cej

Preparation of MoS_2 nanoparticles by a modified hydrothermal method and the photo-catalytic activity of MoS_2/TiO_2 hybrids in photo-oxidation of phenol

Behzad Pourabbas *, Babak Jamshidi

Nanostructured Materials Research Center, Sahand University of Technology, Tabriz 51335-1996, Iran

Received 7 November 2006; received in revised form 19 April 2007; accepted 16 May 2007

Abstract

In this work, a modified hydrothermal method has been developed and employed for synthesis of nanostructured MoS_2 particles. The modification denotes to some changes which were applied with respect to the normal hydrothermal method. Using of a surface-active agent, changing in raw materials and reaction temperature were the main changes which were applied in the modified method with respect to the orginal procedure. Several tools of investigation including XRD, TEM, SEM, and EDXA were used in order to characterize the products and also comparison of the two methods. The results showed a morphology best known as "rag" morphology for the products obtained by both of the methods. In both methods, XRD studies confirmed a semicrystalline state for the particles with slightly lower degree of crystallinity for the modified method. Particle sizes were detected to be in smaller and more uniform state in size and shape for the modified procedure as showed by SEM. Photo-catalytic activity of the particles was checked as MoS_2/TiO_2 hybrids in photo-oxidative removal of phenol as a selected organic compound. Results showed and enhanced photo-catalytic activity for the hybrids with respect to the pure TiO_2 under UV irradiation. MoS_2 nanoparticles also verified to have an enhancement effect on the photo-catalytic activity of TiO_2 under illumination of visible light.

Keywords: Nanoparticles; MoS_2; Photo-catalyst; Photo-oxidation; Phenol

1. Introduction

Molybdenum disulfide MoS_2, has a layered structure like graphite and because of its unique properties, has been known and used in chemical reactions for several years. Among these properties, anisotropy, chemically inertness, photo-corrosion resistance and specific optical properties are included as the superior properties. As a catalyst, MoS_2 carry the advantage of being resistive to poisoning with sulfur and still remain relatively high reactive. MoS_2 is an indirect band gap semiconductor with 1.23 and 1.69 eV band gap energies [1]. Electronic properties of MoS_2 such as position of conductance and valance band has been shown are size dependent due to the quantum size effect with a blue shift in absorption edge upon reduction of particle sizes. Adoption on solar radiation is so that the absorption edge shifts from >1040 to ∼550 nm for a reduction in particle sizes from bulk to 4.5 nm, respectively [2]. So far, three main methods have been developed for the synthesis of MoS_2 nanoparticles: solvothermal [3], hydrothermal [4] and inverse micelle method [5]. Some other different methods include: sonolysis [6], arc [7], plasma microwave [8] and electrochemical/chemical methods [9,10]. In the inverse micelle method, particles are grown inside water containing micelles dispersed in a non-aqueous media. Reaction precursors are usually a molybdenum halide such as $MoCl_4$ and a sulfiding agent such as Na_2S. The advantage is the ability of tuning the particle sizes through controlling the micelle sizes which can be achieved easily by alternation the emulsifier/water ratio. Particles as small as 2.5 nm can be synthesized by this method [5]. Unfortunately, the major drawback for this method is that Mo(IV) halides are not stable compounds and they are not available from chemical supplier companies. Nevertheless, when possible, it can be considered as the best method for the synthesis of semiconducting and other types of nanoparticles. Solvothermal method uses molybdenum trioxide, MoO_3 and elemental sulfur as the starting materials and reaction takes place in a high pressure autoclave at 300 °C in the presence of a reducing agent, hydrazine monohydrate for example. The solvent of the reaction is pyridine. Investigation of the reaction

* Corresponding author. Tel.: +98 411 4249612; fax: +98 411 4249610.
E-mail address: pourabas@sut.ac.ir (B. Pourabbas).

1385-8947/$ – see front matter © 2007 Elsevier B.V. All rights reserved.
doi:10.1016/j.cej.2007.05.028

product by starting different MoO_3/S molar ratios has revealed that crystalline MoS_2 is produced when sulfur content in the reaction mixture is twice or more than that of Mo [3]. Hydrothermal method starts with MoO_3 and NaS_2 in Mo/S molar ratio of 1/3 as the precursor materials and the reaction media is diluted HCl solution. Reaction takes place in an autoclave at temperatures between 200 and 300 °C. It was shown previously that the reaction conditions including temperature, concentration of HCl and presence of some additives are effective on the reaction final product, sizes and morphology of the particles [4]. In the present work, MoS_2 nanoparticles have been synthesized and characterized by a modified hydrothermal method and are compared with the products obtained by the normal hydrothermal method.

One reason for a great interest toward semiconductor metal oxides is their photo-catalytic activity in photo-oxidation reactions especially in the field of water and air treatments [11]. Upon interaction with light, photo-catalysts produce one of the most powerful oxidizing agent $OH^{\bullet}$, which is able to destroy most of organic compounds in aqueous solutions through oxidation-reduction reactions [12]. The advantage of the photo-catalytic oxidative reactions is the ability of the reaction to be carried out under ambient conditions and that usually lead to total mineralization of the organic contaminants. However, they suffer from the drawback of being slow reactions and that photo-oxidation processes took actually long time to be completed result in high costs. Therefore, a large number of works are currently running to improve the efficiency and to adopt the reaction condition to use the advantages of the process [13–15]. Among the several types of semiconductors, TiO_2 has been the most studied compound for its photo-catalytic activity in removal of unwanted organic compounds. TiO_2 is a photostable, non-toxic and cheap white powder which is available easily from many suppliers. In Addition, it has also been shown that TiO_2 has the ability of destruction of a wide range of organic chemicals, which is usually accompanied by total mineralization. However, the principle deficiency of TiO_2 is its absorption edge which falls in UV region at 385 nm (band gap energy 3.0–3.2 eV) [16]. Wavelengths equal or less than this critical value consists only 3% of the sunlight spectrum. For improvement purposes, one approach is the use of hybrid catalysts [17–19]. In this case, two types of semiconductors are used with one of them acting as the supporting material. The combination of two different semiconductors leads to synergic effect and possible electron or hole transfer between electronic states of the two semiconductors. The process prevents the fast electron–hole recombination reaction and therefore, providing additional time for electron or hole to reach to the surface of the photo-catalyst. As a result, the rate of redox reactions increases via the electron–hole lifetime enhancement.

In this work, as is mentioned earlier, nano-sized MoS_2 particles have been synthesized by two different methods, a hydrothermal [4] and a modified hydrothermal method. The latter was a surface-active agent assisted procedure which has been developed in this work. The products of these two methods were characterized and compared by using several means of investigation including XRD, TEM, SEM, and EDAX. After synthesis, and in order to check their photo-catalytic activity, MoS_2 nanoparticles were used as MoS_2/TiO_2 hybrid nano-photo-catalysts in photo-oxidative removal of phenol from aqueous solution. Previously, the effect of crystalline MoS_2 nanoclusters obtained by the inverse micelle technique has been investigated by Wilcoxon et al. [17–19] in pure and also in the form of MoS_2/TiO_2 hybrids in photo-oxidative removal of several water organic pollutants. However, in the present work, the photo-catalytic activity of the MoS_2/TiO_2 hybrids has been investigated by using MoS_2 nanoparticles prepared in this work and compared with Wicoxon's results whenever possible.

2. Experimental

2.1. Materials

Molybdenum trioxide (MoO_3, 99.5%), ammonium heptamolybdate ($(NH_4)_6Mo_7O_{24}{\cdot}4H_2O$, 99.5%), elemental sulfur (99.9%), hydrazine (N_2H_4, 80%), sodium lauryl sulfate (99%), 1-octanol (99.5%), methanol (99.9%) and phenol (99.5%) were purchased from Merck chemical company. Compounds pyridine (99.5%), sodium sulfide (Na_2S, 99.5%) and thiourea (H_2NCSNH_2, 99%) were purchased from Fluka, BDH and Aldrich chemical companies, respectively. Two types of TiO_2 were used in this study which were TiO_2 (P-25) 99.5% from Degussa and TiO_2 (Tiona) 99% from Millenium chemical companies. TiO_2 (P25) is consisted of 80% anatase and 20% of rutile form while TiO_2 (Tiona) is almost completely rutile form.

2.2. Characterization, measurements and the photo-reactor

Powder XRD analysis were performed by using a Simens Kristallflex instrument by scan rate of $0.04^{\circ}\ s^{-1}$ and with Cu Kα ($\lambda = 0.154178$ nm) radiation source. TEM analyses were carried out by using a Philips DM200 electron microscope and the specimens were prepared by sonolysis of the particles in ethanol and drying a drop on a carbon coated copper grid. Analyses of SEM were performed by using a LEO 440i scanning electron microscope equipped with energy-dispersive X-ray analysis (EDXA). Hitachi (D-7000) with UV–vis detector was used for HPLC analyses with a column packed with RP-8 (5 μm).

Photo-catalytic activity of the prepared MoS_2/TiO_2 hybrid catalysts was evaluated according to the photo-oxidative concentration decay of phenol in an aqueous solution. This was carried out in a photo-reactor under irradiation of different light sources, UV and visible. The photo-reactor was consisted of a cylindrical glass batch reactor with a total volume of about 100 ml. Forty millilitre of the total volume was being used in each experiment. It was equipped with a heat exchanger to ensure the solution temperature being constant and a sampling side arm. During the reaction, aliquots of 0.6 ml were being sampled at various irradiation times for phenol concentration analysis. Each sample was filtered using PTFE 0.2 μm syringe filter in order to remove the suspended catalysts; before injection to HPLC. Osram® 400 W xenon lamp was used for experiments under visible light and a

125 W HPK medium-pressure mercury lamp (Philips) for experiments under UV illuminations. The lamp was positioned 6 cm above the top of the reactor and when using visible light, there was a glass placed between top of the reactor and the lamp to work as UV cutoff filter. To prevent catalyst precipitation, all the experiments were carried out under continuous magnetic stirring.

2.3. Preparation of MoS_2 nanoparticles by hydrothermal method

MoO_3 (0.36 g) and Na_2S (1.8 g) were added to 70 ml of 0.4 mol/l HCl aqueous solution in a 100 ml Teflon® lined autoclave reactor. The reaction carried out at 300 °C for 12 h. The black powder product was filtered, washed with ethanol and distilled water and dried at 80 °C under reduced pressure. The products were characterized by using several tools of investigation which are discussed in the following sections. The procedure was adapted to the method describe in Ref. [4].

2.4. Preparation of MoS_2 nanoparticles by the modified hydrothermal method

An aqueous solution of ammonium heptamolybdate, ($(NH_4)_6Mo_7O_{24}\cdot 4H_2O$, 1 g) and thiourea ($H_2NCSNH_2$, 0.9 g), was prepared by dissolving in 50 ml distilled water. 1-Octanol (1.5 ml) and sodium lauryl sulfate (SDS, 0.7 g) was add into a 50 ml Teflon® lined autoclave reaction vessel. The autoclave filled with the aqueous solution up to 75% of its total volume. The autoclave was sealed for annealing under continuous stirring during 5 h at 180 °C. The autoclave was then gradually cooled down to room temperature; and the black precipitate was separated by filtration, washed with ethanol and then by distilled water several times. Finally, it was dried for 6 h at 80 °C under reduced pressure. The products were characterized by several tools of investigation which is discussed in following sections in the text.

2.5. Preparation of MoS_2/TiO_2 hybrid photo-catalysts

Appropriate weights of MoS_2 were dispersed in 300 ml ethanol by using a high speed homogenizer for 20 min in order to disagglomeration and uniform dispersion of the particles in the mixture. TiO_2 (10 g) was then added and homogenizing was continued for additional 15 min. The relative amount of MoS_2 to TiO_2 was adjusted so that the loading level of MoS_2 to be 2, 3 and 5 wt% with respect to the total composition. The suspension was transferred to a rotary evaporator and the solvent was evaporated at 40 °C under reduced pressure. The gray colored precipitates were collected and washed several times with distilled water and then dried for 2 h at 60 °C under vacuum. Two series of MoS_2/TiO_2 hybrid catalysts were prepared by the mentioned procedure by using two types of TiO_2 commercial products: Degussa's TiO_2 (P25) and TiO_2 (Tiona) from Millenium chemical company.

3. Results and discussion

3.1. MoS_2 nanoparticles

3.1.1. Synthesis of MoS_2 nanoparticles

Synthesis of MoS_2 nanoparticles by the hydrothermal method was investigated in different conditions and temperatures between 200 and 300 °C starting by MoO_3 and NaS_2 in Mo/S molar ratio of 1/3. Only the general results are provided here without detailed discussions. Pure crystalline MoS_2 particles were obtained at temperatures between 260 and 300 °C. Increasing HCl concentration from 0.4 to 0.8 mol/l has led to products being contaminated with some other compounds such as MoO_2. Reaction carried out in 0.2 mol/l HCl solution also did not lead to any detectable reaction product. Therefore, 300 °C reaction temperature and 0.4 mol/l HCl concentration was selected for the synthesis of MoS_2 nanoparticles by the hydrothermal method.

In order to reach smaller particles, a modified hydrothermal method of synthesis has been developed in this work. The main applied modification with respect to the normal hydrothermal method was using a surface-active agent in the procedure. The surface-active agent system used in this method was sodium lauryl sulfate (SDS) with 1-octanol as the co-surfactant. Using surface-active agent applied some other changes also with respect to the original procedure. Our early experiments showed that starting from insoluble MoO_3 and Na_2S do not lead to any desired product. Reactions starting with hexacarbonylmolybdate, $Mo(CO)_6$ and elemental sulfur was also frustrated. Finally, soluble ammonium heptamolybdate, $(NH_4)_6Mo_7O_{24}\cdot 4H_2O$ and thiourea were used as successful starting materials in an neutral reaction media. The reaction took place in an autoclave and examined at temperatures between 170 and 210 °C. Below 170 °C no product was obtained. From the other hand, due to thermal decomposition of thiourea, it was impossible to rise the reaction temperature above 210 °C. The products obtained between 170 and 210 °C was determined to be a semicrystalline products. However; the size of the particles investigated to be slightly temperature dependent. By taking all the results into consideration, reaction temperature of 180 °C was concluded to be the optimum reaction temperature in order to obtain pure and uniform nanoparticles of MoS_2.

Characterization and comparison between the products obtained by different methods has been discussed in the following section.

3.1.2. Comparison of MoS_2 nanoparticles obtained by the hydrothermal and modified hydrothermal methods

The SEM micrographs for the products obtained by the hydrothermal method, products of the modified method and the SEM image for the product obtained by the latter method without using surface-active agent are shown in Fig. 1a–c. Particle sizes around 150–200 nm can be estimated from the micrograph for the hydrothermal method while they are smaller (around 100 nm) and more uniform in size and shape for particles of the modified hydrothermal method. It is clear, from Fig. 1c, that the particles are too much bigger and they differ in size and shape extensively. Therefore, it can be concluded that surfactant pre-

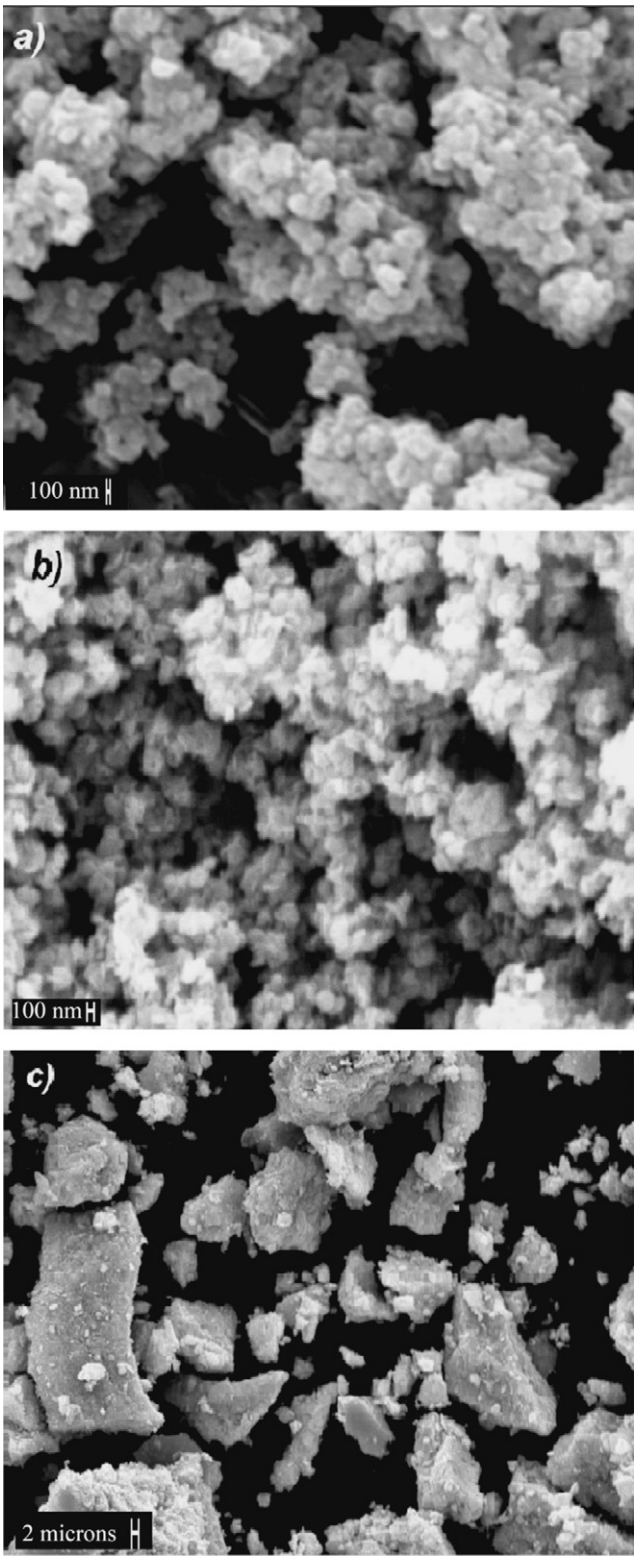

Fig. 1. The SEM micrographs for MoS_2 nanoparticles: (a) obtained by the hydrothermal method, (b) obtained by the modified hydrothermal method and (c) obtained by the hydrothermal method without using surface-active agent.

vents growth of the initially created particles to become larger during the modified hydrothermal method.

Investigation and comparison of the particles by TEM afforded interesting results. The TEM results for the particles obtained by the normal hydrothermal method are shown in Fig. 2 by two magnifications. Ribbon like stacking of S–Mo–S layers are detectable inside the particles. These are completely disordered especially at the corners however, accumulations are seen in core regions of the particles. This describes the morphology mostly known as "rag" morphology. The ribbons have thicknesses approximately 2–3 nm and width of around 100 nm in this morphology. The observed morphology is in complete agreement with results obtained from XRD studies which are discussed in later section. The TEM images of the particles obtained by the modified procedure are shown in Fig. 3. The rag morphology is again the observed morphology for the particles. The main difference, in comparison to Fig. 2, is obviously that the ribbons are much smaller. Very tiny stacks by width of 20–30 nm are seen in the micrographs. This can be attributed to the roll played by the surfactant in reducing the sizes. These are very important properties for particles with catalytic or photocatalytic activities. The first effect is obviously the increase in surface area however, for inorganic semiconductors, the next and maybe the more important is the effect of particle size reduction on electronic and optical properties. The latter for MoS_2 nanoclusters has been discussed in Ref. [4].

The X-ray diffraction pattern, shown in Fig. 4a, is for bulk MoS_2 in its most stable hexagonal crystalline structure [20]. The most important XRD feature which provides a proof for existence of the hexagonal unit cells is the observation of diffraction peaks due to 0 0 2 planes. This is the most prominent peak in Fig. 4a while diffractions from 1 0 0, 1 0 1, and 1 1 0 planes are appeared in smaller intensities. The X-ray diffraction pattern for MoS_2 particles prepared by the normal hydrothermal method is shown in Fig. 4b. Peak 0 0 2 is appeared in its characteristic region $2\theta = 14.5$ as a broad peak. Other detectable peaks are 1 0 0, 1 0 3 and 1 1 0. This combination of the peaks reveals the hexagonal structure for the prepared particles and the broadening of the peaks is in complete agreement with morphological studies and results obtained by TEM. Therefore, and in comparison to the bulk state (Fig. 4a) a semicrystalline structure is assigned for the particles. X-ray diffraction pattern for MoS_2 nanoparticles prepared by the modified hydrothermal method is shown in Fig. 4c. The peak 0 0 2 around $2\theta = 14.5$ is appeared and some peaks due to diffractions from 1 0 0 and 1 1 0 planes are detectable in smaller intensities. In comparison to Fig. 4b, the peaks are broader in some extent, i.e. less crystallinity. This is consistent with the results obtained by TEM. In general, the modified hydrothermal method is accompanied with particles which are smaller and less crystalline in comparison to products obtained by the hydrothermal method.

The purity of the product was determined by quantitative energy dispersive X-ray analysis (EDXA), whose results are shown in Fig. 5a for the products of the modified hydrothermal method. Peaks appeared at 2.2 and 17 keV are due to Mo. The sulfur peak is overlapping with Kα peak of Mo and is not resolvable in the figure. The ratio of Mo/S was detected as 1/1.98 which

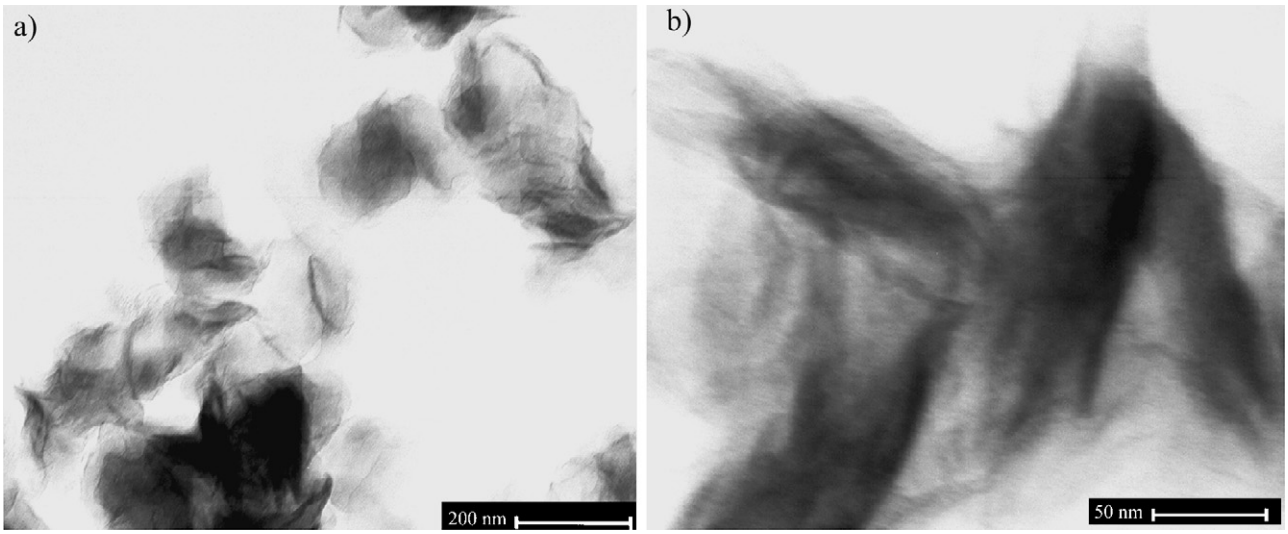

Fig. 2. The TEM images for MoS_2 particles obtained by the normal hydrothermal method, in two magnifications.

is in complete agreement with the chemical formula of MoS_2 showing that no any significant residue of the starting materials or the surfactant is remained in the product.

3.2. MoS_2/TiO_2 hybrids and photo-catalytic activity

3.2.1. The hybrid photo-catalysts

Table 1 describes the compositions of the photo-catalysts prepared in this work and the encoding system. The X-ray diffraction pattern for P25/MH/2 hybrid catalyst is shown in Fig. 5b. The peaks due to MoS_2 are indicated with * mark in the figure. These are in lower intensities due to the low loading level (2%, w/w) of MoS_2 present in the sample and are located in 2θ scale at 15° (0 0 2), 32° (1 0 0), 34° (1 0 2) and 58° (1 1 0). The SEM micrograph for the same sample (P25/MH/2) is presented in Fig. 6. Particles of MoS_2 are appeared as white spots on the surface. Dispersion of these particles is almost uniform and no any significant agglomeration is detectable in the micrograph. The same results were obtained for all other hybrid catalysts prepared in this work.

3.2.2. Photo-catalytic activity of the hybrids

The results obtained for photo-oxidation removal of phenol under visible light illumination are summarized in Fig. 7. It is clear that neither Tiona nor P25 was active in removal of phenol under the applied conditions even after 240 min of reaction time. The result is not surprising because, as mentioned earlier, 3.2 eV band gap energy of TiO_2 fall into the UV region of light spectrum (385 nm) and therefore, it is not expected for TiO_2 to be an active photo-catalyst in visible wavelengths. On the other hand, it was known and has been accepted generally that rutile form of TiO_2 does not show any remarkable photo-catalytic activity. However, Fig. 7 shows that hybrid catalysts P25/MH/2 and T/MH/2 were able to activate the photo-oxidation decomposition of phenol under illumination of visible light. This reveals the synergic effect of MoS_2 and TiO_2 in photo-activity of the hybrid catalysts

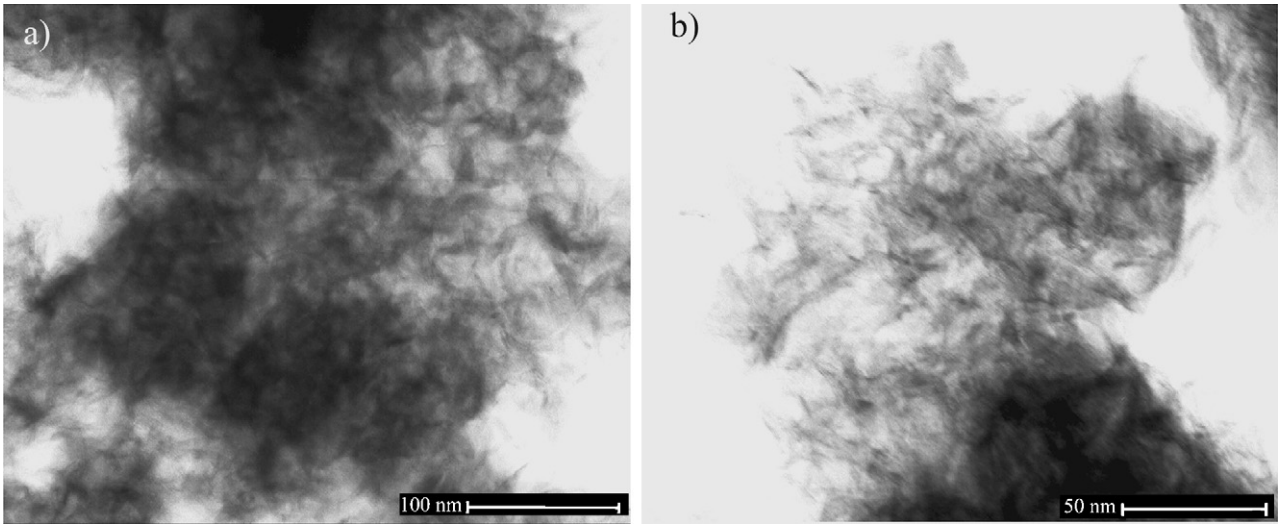

Fig. 3. The TEM images for the particles obtained by the modified hydrothermal method in two magnifications.

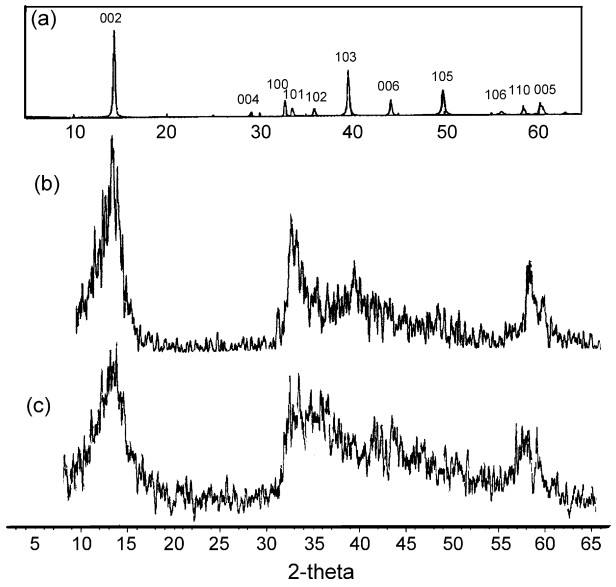

Fig. 4. X-ray diffraction patterns for (a) bulk MoS_2, (b) particles obtained by the hydrothermal method and (c) particles obtained by the modified hydrothermal method.

Table 1
Encoding system for the compounds used or prepared in this work

Sample	Type of TiO_2	Type of MoS_2	MoS_2 loading level (wt%)
P25	P25[a]	–	0
T	Tiona[b]	–	0
P25/MH/2	P25	MH[c]	2
P25/MH/3	P25	MH	3
P25/MH/5	P25	MH	5
P25/H/2	P25	H[d]	2
P25/H/3	P25	H	3
P25/H/5	P25	H	5
T/MH/2	Tiona	MH	2
T/MH/3	Tiona	MH	3
T/MH/5	Tiona	MH	5
T/H/2	Tiona	H	2
T/H/3	Tiona	H	3
T/H/5	Tiona	H	5

[a] TiO_2 P25, from Degussa 80% anatase and 20% rutile.
[b] TiO_2, Tiona from Millenium > 99% rutile.
[c] Prepared by the modified hydrothermal method.
[d] Prepared by the normal hydrothermal method.

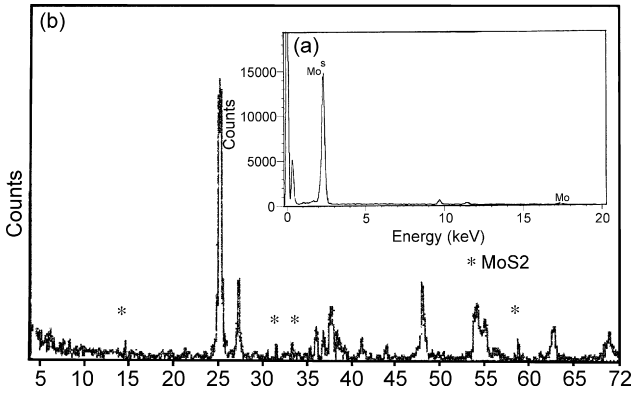

Fig. 5. (a) Energy dispersive X-ray analysis (EDXA) result for MoS_2 particles obtained by the modified hydrothermal method, (b) X-ray diffraction pattern for P25/MH/2 hybrid catalyst.

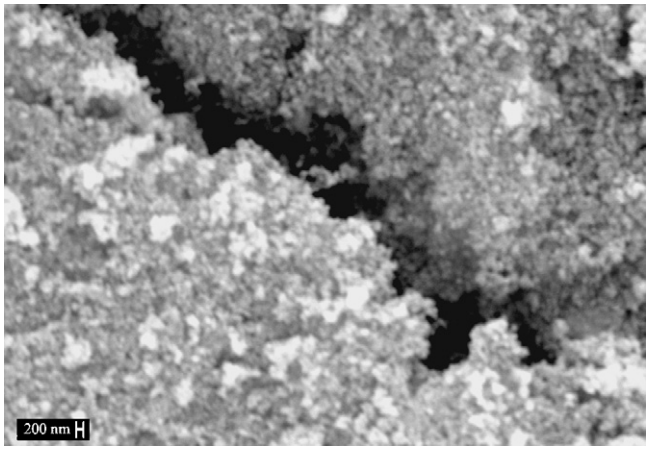

Fig. 6. The SEM micrograph for P25/MH/2 hybrid catalyst.

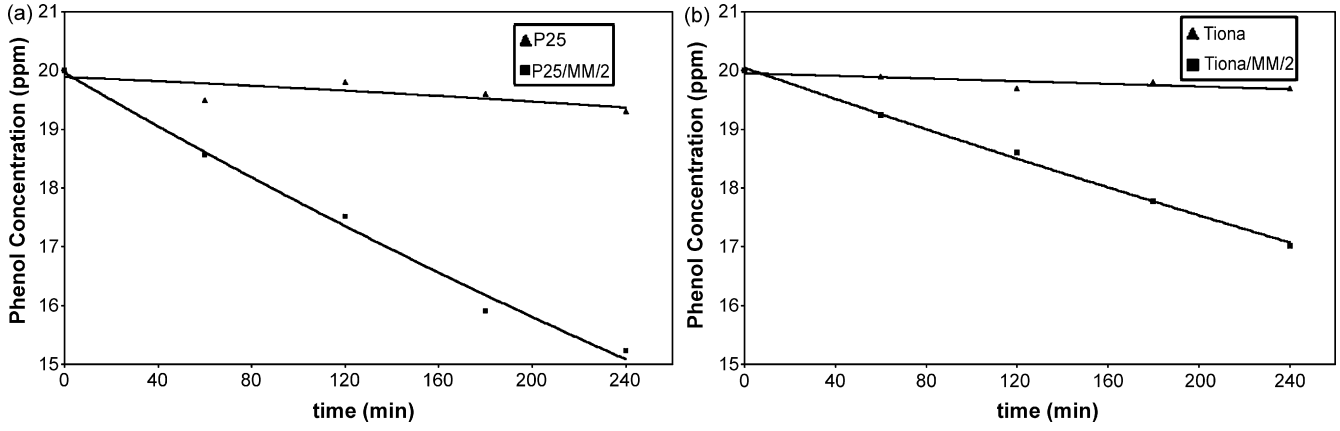

Fig. 7. Concentration-irradiation time diagrams for photo-oxidative removal of phenol under illumination of visible light, (a) in the case of using P25 and P25/MH/2 hybrid catalyst, and (b) in the case of using Tiona and Tiona/MH/2.

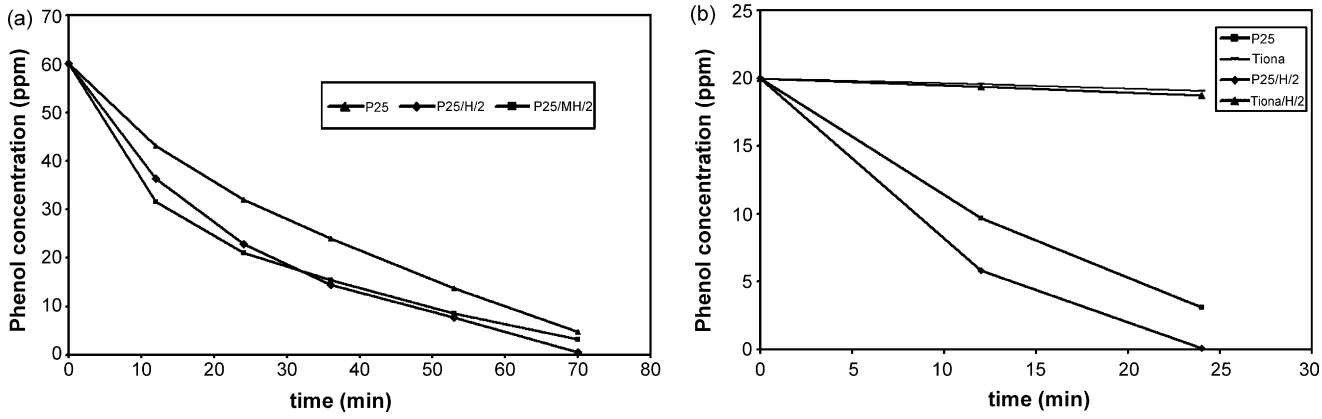

Fig. 8. Photo-oxidative decline of phenol concentration under UV illumination of light. (a) Photo-catalytic activity for P25, P25/MH/2 and P25/H/2, and (b) the effect of TiO_2 type.

clearly. It is an amazing result that not only P25 but also Tiona based hybrid has acquired a photo-catalytic activity due to presence of MoS_2 in the composition. It has been shown previously by Wilcoxon [17,18] that 4.5 nm nanoclusters of MoS_2 to be an active photo-catalyst in removal of phenol even under visible wavelengths of light. Our results show that not only in pure form but also in hybrid with TiO_2, MoS_2 has the visible light photo-catalytic activity. It is worthy to note that, MoS_2 particles in this work were different in synthesis and characteristics with those employed by Wilcoxon. We also used particles without further purification or partitionation into narrow width particle size distribution.

The experimental results for the photo-oxidative decline of phenol concentration under UV illumination can be seen in Fig. 8. The photo-catalytic activity of P25, P25/MH/2 and P25/H/2 are compared in Fig. 8a. A relatively high photo-catalytic activity is seen for both of the photo-catalysts so that phenol has been removed almost completely after 70 min from 60 ppm initial concentration. Meanwhile, higher initial rates of decomposition are seen for the hybrid catalysts with a slightly higher activity for P25/MH/2 in comparison to P25/H/2. The effect of TiO_2 type on the photo-oxidative decay of phenol under UV illumination is shown in Fig. 8b. Neither Tiona nor T/H/2 has shown a significant photo-catalytic activity under UV condition for removal of phenol. However, the phenol concentration is declined from 20 ppm initial concentration to almost zero after 25 min by using P25 or P25/H/2. A higher rate of photo-oxidation is observed for P25/H/2 in comparison to pure P25. The photo-catalytic activity in the prepared hybrid catalysts was observed to be dependent to the loading level of MoS_2 in the hybrids. The photo-catalytic activity of the hybrids with different loading level of MoS_2 are compared with pure P25 (UV illumination) in Fig. 9. As can be seen, the photo-catalytic activity is

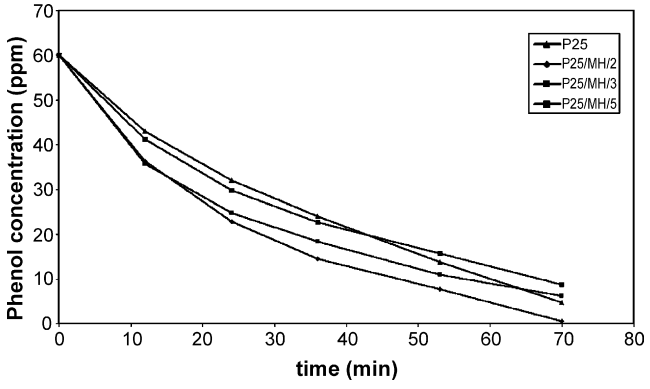

Fig. 9. The effect of MoS_2 loading level on the photo-catalytic activity of the hybrids with respect to pure P25 (UV illumination).

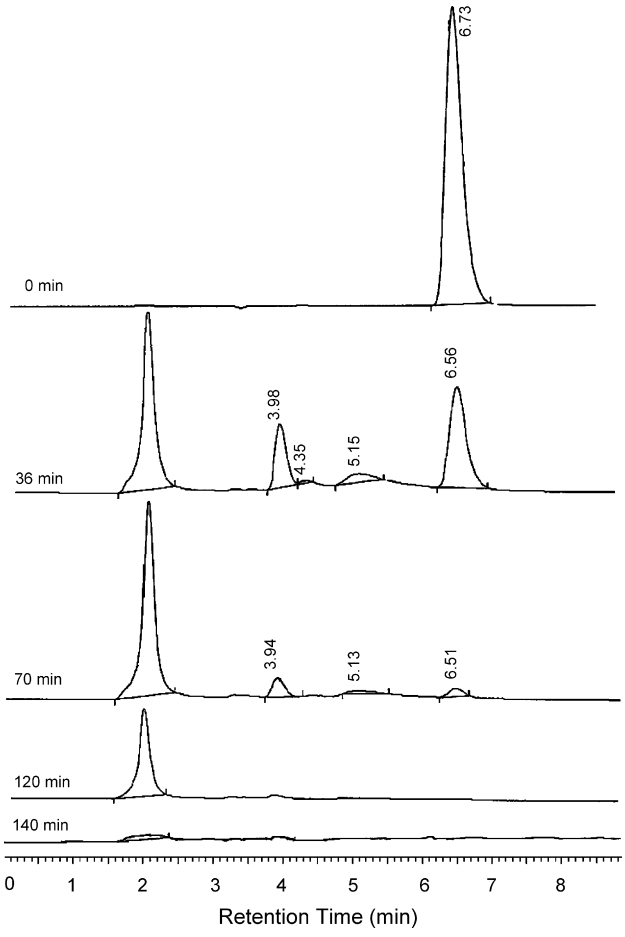

Fig. 10. HPLC elution peaks between 0 and 145 min of irradiation time for the case ofusing P25/MH/2 as the photo-catalyst under irradiation of UV light.

decreased in the hybrid series by increasing the weight percent loading of MoS_2 from 2 to 5 wt%. Higher initial photo-oxidation rates for the hybrids in comparison to P25 are in descending order with increasing MoS_2 content. As reaction proceeds, these rates slow down leading to a higher phenol residual concentration after 70 min elapsed reaction time. For hybrids P25/H/3 and P25/H/5 the residual concentration finally reaches to a higher amount accompanied with pure P25. The same behavior also observed and reported by Wilcoxon suggesting the electron or hole transfer occurring between TiO_2 and MoS_2 nanoparticles. This leads to an improved charge separation which helps photo-oxidation process. Therefore, this synergic effect reaches to a maximum around 2.5% loading of MoS_2 in the hybrids.

HPLC chromatograms provided evidences for the complete mineralization of phenol during the photo-oxidation reaction. The HPLC elution peaks are shown in Fig. 10 between 0 and 145 min of irradiation time which was being carried out by using P25/MH/2 for a 60 ppm aqueous solution of phenol under irradiation of UV light. The peak at 6.6 min retention time is due to phenol and as can be seen its area is reducing with reaction time. As reaction proceeds, some new peaks are appeared in the HPLC chromatograms mainly at 2.1, 4 and 5.1 elution times. These are attributed to the photo-oxidation reaction intermediate compounds of phenol. The chromatogram after 145 min shows the complete removal of all the organic compounds and that the total mineralization is occurred.

4. Conclusion

Synthesis of MoS_2 nanoparticles is of interest because of its photo-catalytic activity in photo-oxidation removal of organic compounds. In the modified hydrothermal method of synthesis, the surface-active agent prevents further growth of the particles and helps to obtain particles with more uniform shapes and size. The rag morphology remain unchanged however, the ribbons are much smaller in the case of the modified hydrothermal method. The photo-catalytic investigations showed that both types of MoS_2 nanoparticles obtained by the two methods show a synergic effect in photo-catalytic activity of the TiO_2 hybrids. In experiments, slightly higher rates of photo-oxidation reactions were observed for the MoS_2 particles obtained by the modified method.

In comparison to previous works, the results showed that MoS_2 nanoparticles retain their photo-catalytic activity even if there are not purified or separated into narrow width of particle sizes.

References

[1] X. Bokhimi, J.A. Toledo, J. Navarette, X.C. Sun, M. Portilla, Thermal evaluation in air and argon of nanocrystalline MoS_2 synthesized under hydrothermal conditions, Int. J. Hydrogen Energy 26 (2001) 1271–1277.

[2] J.P. Wilcoxon, T.R. Thurston, J.E. Martin, Applications of metal and semiconductors nanostructures as thermal and photo-catalysts, Nanostruct. Mater. 12 (1999) 993–997.

[3] J.H. Zhan, Z.D. Zhang, X.F. Qian, C. Wang, Y. Xie, T. Qian, Solvothermal synthesis of nanocrystalline MoS_2 from MoO_3 and elemental sulfur, J. Solid State Chem. 141 (1998) 270–273.

[4] W.J. Li, E.W. Shi, Z.Z. Chen, H. Ogino, T. Fukuda, Hydrothermal synthesis of MoS_2 nanowires, J. Cryst. Growth 250 (2003) 418–422.

[5] J.P. Wilcoxon, P.P. Newcomer, G.A. Samara, Synthesis and optical properties of MoS_2 and isomorphous nanoclusters in the quantum confinement regime, J. Appl. Phys. 81 (1997) 7934–7944.

[6] Q. Li, J.T. Newberg, J.C. Walter, R.M. Penner, Polycrystalline molybdenum disulfide (2H-MoS_2) nano- and microribbons by electrochemical/chemical synthesis, Nano Lett. 4 (2004) 277–281.

[7] N. Sano, H. Wang, M. Chhowalla, I. Alexandrou, G.A.J. Amaratunga, M. Natio, T. Kanki, Fabrication of inorganic molybdenum disulfide fullerenes by arc in water, Chem. Phys. Lett. 368 (2003) 331–337.

[8] D. Vollath, D.V. Szabo, Synthesis of nanocrystalline MoS_2 and WS_2 in a microwave plasma, Mater. Lett. 35 (1998) 236–244.

[9] M.P. Zach, K. Inazu, K.H. Ng, J.C. Hemmingr, R.M. Penner, Synthesis of molybdenum nanowires with millimeter-scale length using electrochemical step edge decoration, Chem. Mater. 14 (2002) 3206–3216.

[10] Q. Li, E.C. Walter, W.E. van der Veer, B. Murray, J.T. Newberg, E.W. Bohannan, J.A. Switzer, J.C. Hemminger, R.M. Penner, Molybdenum disulfide nanowires and nanoribbons by electrochemical/chemical synthesis, J. Phys. Chem. B 109 (2005) 3169–3182.

[11] N.H. Salah, M. Bouhelassa, S. Bekkouche, A. Boultii, Study of photocatalytic degradation of phenol, Desalination 166 (2004) 347–354.

[12] M. Peiro, J.A. Ayllon, J. Peral, X. Domenech, TiO_2-photocatalyzed degradation of phenol and *ortho*-substituted phenolic compounds, Appl. Catal. B: Environ. 30 (2001) 359–373.

[13] Z. Wang, W. Cai, X. Hong, X. Zhao, F. Xu, C. Cai, Photocatalytic degradation of phenol in aqueous nitrogen-doped TiO_2 suspensions with various light sources, Appl. Catal. B 57 (2005) 223–231.

[14] F. Kiriakidou, D.I. Kondarides, X.E. Verykios, The effect of operational parameters and TiO_2-doping on the photocatalytic degradation of azo-dyes, Catal. Today 54 (1999) 119–130.

[15] W. Han, W. Zhu, P. Zhang, Y. Zhang, L. Li, Photocatalytic degradation of phenols in aqueous solution under irradiation of 254 and 185 nm UV light, Catal. Today 90 (2004) 319–324.

[16] D. Chatterjee, A. Mahata, Visible light induced photodegradation of organic pollutants on dye adsorbed TiO_2 surface, J. Photochem. Photobiol. A 153 (2002) 199–204.

[17] J.P. Wilcoxon, T.R. Thurston, J.E. Martin, Applications of metal and semiconductor nanoclusters as thermal and photo-catalysts, Nanostruct. Mater. 12 (1999) 993–997.

[18] J.P. Wilcoxon, Photo-oxidation method using MoS_2 nanocluster materials, US Patent 6,245,200 (2001).

[19] T. Thurston, J.P. Wilcoxon, Photooxidation of organic chemicals catalyzed by nanoscale MoS_2, J. Phys. Chem. B 103 (1999) 11–17.

[20] Y. Peng, Z. Meng, C. Zhong, J. Lu, W. Yu, Z. Yang, Y. Qian, Hydrothermal synthesis of MoS_2 and its pressure-related crystallization, J. Solid State Chem. 159 (2001) 170–173.